Colloids and Surfaces A: Physicochemical and Engineering Aspects 677 (2023) 132413

Contents lists available at ScienceDirect

Colloids and Surfaces A: Physicochemical and Engineering Aspects

journal homepage: www.elsevier.com/locate/colsurfa

Polymer-nanoparticle thin scaffolds with any-shape magnetic field gradients

Tomasz Mazur[a,1], Łukasz Mazur[b,1], Mariusz Borkowski[c], Tomasz Kuciel[d], Michał Szuwarzyński[a,*]

[a] AGH University of Science and Technology, Academic Centre for Materials and Nanotechnology, Mickiewicza 30, 30-059 Krakow, Poland
[b] AGH University of Science and Technology, Faculty of Materials Science and Ceramics, Mickiewicza 30, 30-059 Krakow, Poland
[c] Polish Academy of Sciences, Jerzy Haber Institute of Catalysis and Surface Chemistry, Niezapominajek 8, 30-239 Krakow, Poland
[d] Jagiellonian University, Faculty of Chemistry, Gronostajowa 2, 30-387 Krakow, Poland

GRAPHICAL ABSTRACT

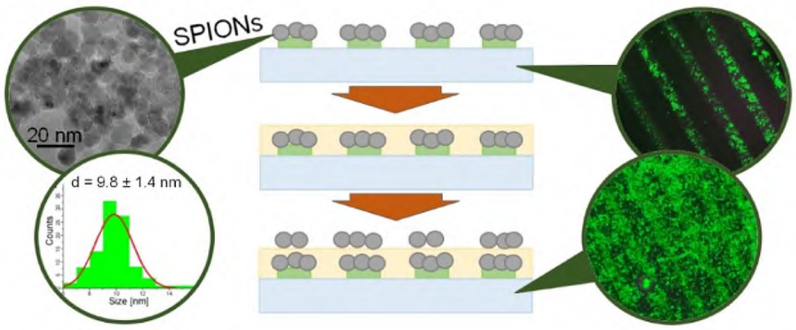

ARTICLE INFO

Keywords:
Nanoparticles
Magnetic scaffolds
SPIONs
Self-assembly
Polymer composites

ABSTRACT

This study investigates the self-assembly of magnetic nanoparticles into a flat nanocomposite surface with concealed magnetic patterns. The application of a multilayer stamping medium and the presence of a magnetic field gradient would enable the attraction and organization of superparamagnetic iron oxide nanoparticles (SPIONs) onto predefined areas, corresponding to a pre-fabricated magnetic layer. The experimental approach involved preparing patterned surfaces by applying a multilayer of poly(ethyleneimine) (PEI) and poly(styrene sulfonate) (PSS) as a stamping medium. The SPIONs selectively adhered to the surface, mirroring the underlying magnetic layer shape. Subsequently, these SPION were subjected to an 80 °C treatment in the presence of an external magnetic field to enhance their magnetic properties, and then covered with a polystyrene layer. Using atomic force microscopy, magnetic force microscopy and dark field mode optical microscopy we demonstrated that obtained patterned magnetic field gradients are strong enough to attract and organize magnetic material on top of them, even when being covered with polymeric layers. Moreover, our findings show that the oriented deposition of magnetic nanoparticles is primarily determined by the strength of magnetic interactions between

* Corresponding author.
E-mail address: szuwarzy@agh.edu.pl (M. Szuwarzyński).
[1] These authors contributed equally.

https://doi.org/10.1016/j.colsurfa.2023.132413
Received 3 July 2023; Received in revised form 5 September 2023; Accepted 12 September 2023
Available online 17 September 2023

the pattern and nanoparticles, independently of surface topography (with roughness of 0.21 ± 0.06 nm) or Brownian motions.

1. Introduction

Self-assembly is one of the easiest and most inexpensive ways to organize nanoparticles into more complicated, well-organized structures. Understanding assembly mechanisms is crucial for developing new surface functionalization techniques and at the same time opens yet unexplored pathways leading directly towards novel materials discovery and device production. [1] Among many types of structures suitable for self-assembly, magnetic nano- and microparticles, due to their ability to generate subtle and precise field gradients, are of particular interest contributing to development of novel techniques [2]. This interest exists not only in relation to magnetic interactions between particles, but also due to their susceptibility to the external magnetic fields. The magnetic properties of such particles can be applied in many fields such as drug delivery [3], cancer treatment [4], data storage [5], advanced cell cultures [6], cellular manipulation [7], high energy storage [8] or substance targeting [9]. Moreover, magnetic nanoparticles in the presence of an external magnetic field, can be used as building blocks in large-area nanostructurization and self-assembly techniques [10,11] resulting in novel materials discoveries [12–14]. Regarding their constitution, magnetic nanoparticles can be created from metals, metal oxides and composites [15–17]. For the last two decades a growing interest in magnetic nanoparticles was focused mainly on iron oxide particles (SPIONs) due to their superparamagnetic properties [18]. In particular, SPIONs have found applications in biological and biomedical applications, mainly as contrast agent in magnetic resonance imagining. [19,20].

The self-assembly of magnetic nanoparticles into patterned nanostructures gained even more interest in previous years. This spike of attention is mostly due to the fields of magnetic storage devices which offer better performance and higher storage capabilities [21], biosensors with very high sensitivity [22], and magnetic random access memories, which are capable of the store data in magnetic domains instead an electric charge [23]. One of the challenges with utilizing the technological application of patterned magnetic nanostructures is the development of self-assembly bottom-up approaches that allow for the organization of nanoparticles into aggregates with precisely controlled shapes, structures, sizes and positions on the substrate. So far, controlled self-assembly at the interface was obtained using external forces like a strong magnetic field [24–26]. Such an approach allows for the precise deposition of magnetic nanoparticles and their local arrangement through the manipulation of the external magnetic field only [27–29]. However, practice shows, there are considerable problems with the generation of complex and well-controlled magnetic fields, required in the self-assembly of nano-objects. Typically, sophisticated apparatus and multi-step procedures are required for the patterning of solid substrates [26,30,31]. This level of complexity elevates overall costs of the nano-devices fabrication processes. Due to this fact, alternative self-assembly methods that utilized template-assisted deposition of nanoparticles into patterns were developed. This group of techniques utilizes a variety of phenomena such as electrostatic interactions between oppositely charged nanoparticles and patterned surfaces [32,33] or de-wetting aqueous dispersions [34,35]. However, template-assistant methods exhibit some shortcomings in terms of orientation control, precision of assembly and scalability [36]. The main self-assembly procedures of magnetic nanoparticles can be limited to production of 1D chains, 2D monolayers and 3D cuboids [37] like ring-trapped in microelectromagnet matrix nanoparticle clusters [38], magnetic-nonmagnetic composites [39], oriented polymer matrix working as assembly environment [40,41] or surface templates for the self-assembly of nanoparticles after the spin-coating method [42].

In this work we present a novel approach towards controlled organization of nanoparticles on flat surfaces. Our method leads to formation of hybrid template-assisted magnetic surface for self-assembly of SPIONs into the pre-designed patterns directly on the polymeric surface. Firstly, by using electrostatic interactions, we formed a pattern from SPIONs on a silicon surface. The patterns were subjected to elevated temperatures inside a laboratory oven and were concurrently positioned between stationary magnets. This arrangement generated an external magnetic field that, in turn, exerted an influence on the ultimate alignment of magnetic domains. [43,44] These magnetic patterns were then covered with a thin layer of polystyrene, a known good polymeric nonmagnetic coating, resulting in low-roughness surfaces. [45,46] Next, we provided proofs that obtained patterned magnetic field gradients are strong enough to attract and organize magnetic nanoparticles on top of polymeric layer. Through various means, we successfully constructed a magnetic structure capable of both magnetization and harnessing its self-generated magnetic field gradient to manipulate nanoscopic objects.

2. Experimental section

2.1. Materials

Positive photoresist (Allresist, AR-P 3700 series) was purchased from POCH (Avantor, Gliwice, Poland). Polydimethylsiloxane (PDMS) was purchased from Dow Corning under the name Sylgard 184 Silicone Elastomer Kit. Iron(III) chloride hexahydrate (p.a.), and iron(II) chloride tetrahydrate (p.a.) were purchased from Sigma Aldrich (St. Louis, MO, USA). Ammonium hydroxide (25 %, p.a.) was purchased from Chempur (Piekary Slaskie, Poland). Polyethyleneimine (PEI, 50 % (W/v) aqueous solution, M_n ~60,000 Da and poly(sodium 4-styrene sulfonate) (PSS, average M_w ~ 70,000 Da) were purchased from Sigma-Aldrich. Polystyrene (PS, M_w = 9880 Da, PDI = 1.04) was purchased from PSS GmbH (Mainz, Germany). All products were used without further purification. Polyelectrolyte solutions were prepared in HPLC-grade water from Sigma-Aldrich to prevent contamination and ionic effects. For other steps, water from the Hydrolab HLP 10UV water system was used.

2.2. Methods

Atomic force microscope (AFM) topography images were obtained with Dimension Icon XR microscope (Bruker, Santa Barbara, CA, USA) working in the air in the PeakForce Tapping (PFT) mode, using standard silicon cantilevers of a nominal spring constant of 0.4 N/m and triangular geometry tip, nominal tip radius of 2 nm. Magnetic force microscope (MFM) images were acquired using the same microscope and magnetic Co/Cr coated silicon cantilevers of a nominal spring constant of 2 N/m. The MFM images were captured in the lift mode at 200 nm lift height for the scaffolds and 100 nm lift height for the bare nanoparticles. The cantilevers were magnetized with a small magnet for 30 s with a constant magnet-tip distance (1 mm) before the measurements. Dynamic light scattering (DLS) technique was used to determine the sizes and zeta potentials of the nanoparticles (Malvern Nano ZS light-scattering apparatus; measurements at 173° scattering angle, 25 °C). The aqueous dispersion of SPIONs was exposed to a 633 nm laser and the time-dependent autocorrelation function of the photocurrent was acquired every 10 s, with 15 acquisitions for each run. The z-averaged mean diameters, polydispersity, and distribution profiles of the sample were gathered using Malvern software. The zeta potential measurements were made using the Laser Doppler Velocimetry technique (LDV). The structures and morphologies of the prepared patterns were studied with NIKON Eclipse LV150N optical microscope in the dark field mode (DF).

Moreover, the shape and the size of the nanoparticles were determined using a Tecnai TF 20 X-TWIN (FEI, Hillsboro, OR, USA) transmission electron microscope (TEM).

2.3. Synthesis of Fe_3O_4 nanoparticles (SPIONs)

The syntheses of SPIONs nanoparticles were performed by coprecipitation of 0.1622 g $FeCl_3 \cdot 6H_2O$ and 0.0596 g $FeCl_2 \cdot 4H_2O$ in an aqueous medium (the molar ratio of ions Fe(III): Fe(II) = 2:1, solution pH≈ 2) according to the method described previously. [47,48] After the deoxygenation, by purging with argon, the solution was sonicated for 10 min (1 s pulse per every 5 s) in a thermostatic bath at 20 °C (Sonic-6, Polsonic, 480 W). Subsequently, nanoparticles were precipitated by dropwise addition of the 5 ml of 5 M NH_3(aq), and the suspension of the formed nanoparticles (see Fig. 1.A.) was further sonicated for 30 min. To purify the obtained dispersion magnetic chromatography was performed.

2.4. Replica mold masters preparation

The silicon (2 × 2 cm, Siegert Wafer) replica mold masters were prepared in the cleanroom of class 100 (AGH UST, Academic Centre for Materials and Nanotechnology, Krakow, Poland) equipped with maskless MicroWriter ML3 Pro (385 nm light source). The radiation dose for this process was established at 140 mJ/cm^2. Klayout free software was utilized for the design of the patterns. The process of replica mold masters development was started by washing silicon substrates with acetone in an ultrasonic bath for 10 min at 50 °C. After drying with N_2, the same procedure was repeated but with the methanol. After finishing the cleaning procedure, silicon substrates were placed on a hot plate

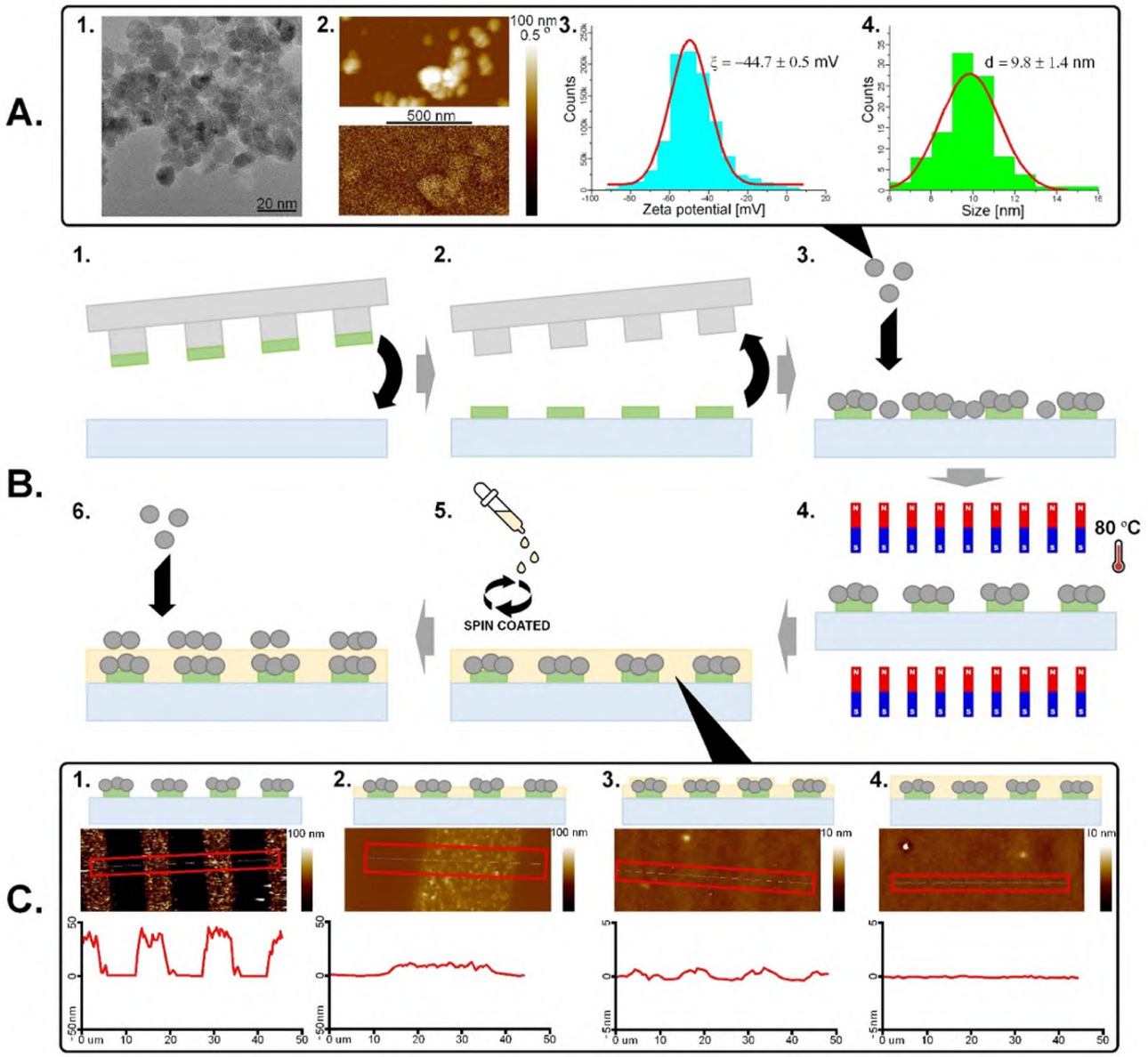

Fig. 1. A. Characterization of SPIONs: 1. TEM image, 2. AFM topography image (top) with MFM phase image (bottom), 3. Zeta potential histogram, 4. TEM size distribution histogram; B. fabrication of magnetic patterns on a silicon surface: (1.) Polyelectrolyte adsorption on the PDMS stamp with the desired microstructures using replica molding, (2.) Transfer of polyelectrolyte layer onto a silicon surface, (3.) Controlled deposition of magnetic SPIONs, (4.) Heating patterned surfaces in the magnetic field, (5.) Controlled spin-coating of polystyrene, (6.) the second deposition of SPIONs; C. AFM topography images with corresponding cross-sections during optimization of polystyrene coating process using the spin-coating technique: 1. bare patterned SPIONs, 2. Patterned SPIONs after spin coating with 2500 rpm 3. Patterned SPIONs after spin coating with 2000 rpm, 4. Patterned SPIONs after spin coating with 1500 rpm.

(100 °C) for one minute and then immediately transferred to a spin-coater. A Pasteur pipette was used for adding a few droplets of the photoresist to form a thin layer across the silicon substrate. Then, the photoresist was evenly distributed by spin coating with given parameters: time – 45 sec, RPMs - 6000. Silicon substrate with a thin photoresist layer was then placed on a hot plate (100 °C) for one minute. The prepared substrate was transferred to the MicroWriter ML3 Pro device, for UV exposure. After the process was finished, the silicon substrate was immersed in the developer for around ten seconds and then transferred immediately in distilled water and left for 30 s. Finally, replica mold masters were cured on a hot plate (115 °C) for one minute.

2.5. Preparation of the PDMS stamps

Replica mold masters with the previously designed patterns were put under a static vacuum in a desiccator with 50 μL of trichloro(1,1,2,2-perfluorooctyl)silane - silanizing agent - for 30 min. PDMS resin was mixed with a hardener in a ratio of 10:1 by weight. Then, such a mixture was introduced into replica mold masters and left in a dryer for 12 h at 70 °C. After this process, PDMS stamps were cut out from replica mold masters.

2.6. Preparation of patterned surfaces

Before the preparation of patterned silicon substrates, clean substrates were cleaned for 15 min in oxygen plasma. PDMS stamps were immersed in polyelectrolyte solutions starting from polyethyleneimine (PEI), then poly(sodium 4-styrene sulfonate) (PSS) solution, and finally again in PEI. The concentration of the solutions was established at 1 mg·ml^{-1}. The time of immersion for all polyelectrolyte solutions was 10 min. Between the solution changes, PDMS stamps were cleaned in distilled water for one minute in an ultrasonic bath. After the last cleaning, the stamps were dried in argon. As a result, the PDMS stamp was covered with three layers of assembled polyelectrolytes nanofilms, Transfer of these layer from the stamp onto the silicon substrate involves heating the substrate to 90 °C, and placing the stamps with the pattern facing the substrate (see Fig. 1.B.1.). Then, the stamp was gently pressed and left for 20 min. After that time, stamps were removed from the silicon substrate leaving the transferred pattern on the surface (see Fig. 1.B.2.).

2.7. Deposition of SPIONs on patterned polyelectrolytes

For further deposition of the Fe_3O_4 nanoparticles (SPIONs) on the patterned substrate (see Fig. 1.B.3.), they were immersed in Fe_3O_4 nanoparticles solution for five minutes. After that time, substrates were removed from the nanoparticle solution, immersed in distilled water, and dried with argon. As a result of this step, patterns of deposited Fe_3O_4 nanoparticles can be observed, in the areas where previously polyelectrolyte films were transferred.

2.8. Heating the SPIONs patterned samples under the magnetic field

To enhance the magnetic response of patterned nanoparticles, samples were placed in a specially designed holder in the oven for 1 h at 80 °C (see Fig. 1.B.4.). Holder was made of two neodymium magnets (N35 magnet, 45 mm (l), 25 mm (w), 10 mm (h), B = 0263 T in the geometric center of the surface of the magnetic pole) placed above and under the sample with a 2 mm distance between them.

2.9. Fabrication of patterned PS magnetic scaffolds

After obtaining patterned magnetic scaffolds on the substrate surface, they were covered with thin layer of polystyrene (see Fig. 1.B.5.). For this purpose polystyrene (M_w = 9880 Da) was dissolved in toluene, to obtain a concentration of 120 mg/ml. Then, substrates with magnetic patterns were placed in a spin coater. The dynamic mode was used for the deposition of polystyrene coating with the following parameters: time – 45 sonds, rpm – 1500. After this process, substrates with magnetic patterns coated with PS thin film were placed on a hot plate (70 °C), to remove remaining solvent. This step allows for complete coverage of Fe_3O_4 nanoparticles by PS thin film.

2.10. Controlled assembly of SPIONs on PS magnetic scaffolds

The assembly of second SPIONs layer, placed on top of the PS surface (see Fig. 1.B.6.), was carried out in an analog way as it was done in similar wat to the first nanoparticles deposition step directly polyelectrolyte patterned substrates. Plates with PS coatings covering magnetic patterns were immersed in SPIONs solution for 24 h then and then gently immersed in a flask with distilled water and nextly dried in an oven at 50 °C for 30 min to evaporate all residual water. No water flush or gas flow were used for washing, in order to protect the obtained surface nanoparticle assemblies from the uncontrolled shift. The holding force was based on surface magnetic field gradients rather than adhesive effects.

3. Results and discussion

3.1. SPIONs characterization

In presented research, we decided to use superparamagnetic iron oxide nanoparticles (SPIONs) synthesized by the coprecipitation method of respective iron salts in an aqueous medium. The selection of SPIONs was motivated by following attributes: robust stability, uniform particle size distribution, and a sufficiently high surface potential. Each of these characteristics contributed to the improvement in the quality of the generated patterns. Method of synthesis was validated before [36] and yields nanoparticles with low polydisperisbility, well-defined shapes and diameters of 9.8 ± 1.4 nm (TEM image - Fig. 1.A.1, DLS size statistics – Fig. 1.A.4.), strong magnetic properties (confirmed by magnetic force microscopy - Fig. 1.A.2.) and strong negatively charged surface (zeta potential, $\xi = -44.7 \pm 0.5$ mV) – making the dispersion stable in time (Fig. 1.A.3.).

3.2. Fabrication and characterization of SPIONs patterned surfaces with PS coating

In order to fabricate SPIONs patterned surfaces with PS coating on a flat silicon surface, firstly polyelectrolyte multi-layer, consisting of three alternating layers of PEI (polyethyleneimine), PSS (poly(sodium 4-styrene sulfonate)) and PEI, was mechanically transferred from a PDMS replica mold onto a cleaned surface of silicon. The usage of a triple layer stabilizes the 2-D shape of the patterned structure and keeps the top PEI positively charged layer, evenly-distributed throughout whole surface of PDMS stamp. In the next step silicon substrate with the PEI-PSS-PEI pattern was immersed for 5 min in a solution of SPIONs. The resulting hybrid polyelectrolyte-nanoparticles pattern was subsequently washed with H_2O and dried in argon. The average thickness of obtained homogeneous hybrid layer was 41.5 ± 3.1 nm (see Fig. 1.C.1.). The obtained hybrid layers are homogeneous and form structures with low roughness (R_q < 12 nm). This is mostly due to the small size and low polydispersity of SPIONs, well-formed PEI-PSS-PEI layer and also strong attraction between negatively charged SPIONs and positively charged top PEI polyelectrolyte pattern. Patterned substrates with nanoparticles were placed in the static magnetic field (neodymium magnets) in the oven for 1 h at 80 °C. Placing nanoparticles in a constant magnetic field at elevated temperature caused the organization of magnetic moments of SPIONs [42], giving a better magnetic response of the prepared substrate. The latter is crucial in the next step, which is another round of SPIONs deposition, this time on the PS coating. The magnetic response of SPIONs, both untreated and heat treated, on polyelectrolyte patterned

substrate was studied using magnetic force microscopy (MFM) and is shown in Fig. 2. A and 2.B. It is clearly visible that the MFM image of the magnetic phase is different after treating the substrates in the oven. What should be underlined, is the fact that tip magnetization procedure and scanning parameters in both cases were exactly the same. For all measurements the same series of magnetic Co/Cr coated silicon probes was used, the exact value of lift distance of 200 nm during interleave scanning mode, exact magnetization procedure in the dedicated holder (Bruker) with a small ferrite magnet, constant magnet-tip distance (1 mm) and magnetization time set for 30 s. Similarity of the treatment and measuring conditions leads to the conclusion, that the difference in the MFM magnetic phases comes from the changes in magnetization of each individual of the SPIONs. The observed increase in magnetization of SPIONs is likely a result of the reorientation of nanoparticles or magnetic domains within the nanoparticles when exposed to an external magnetic field at higher temperatures. In the context of pattern-oriented applications, traditional magnetization measurements were not conducted, but instead, the magnetic mode of AFM. The latter proved sufficed to properly depict and provide a rough quantification of the direction change in magnetization for the nanoparticles on the surface. The phenomena of magnetization changes for self-assembled structures needs further clarification, is however out of scope of current research.

The presented MFM magnetic phase signal was measured at higher distances, 1000 nm and 2000 nm, to prove micrometer range of magnetic interactions. As it was excepted and is shown in Fig. 2.B., the intensity of MFM response is weaker at 2000 nm lift distance, compared to 200 nm. It is still measureable, which is a good omen, that covering the paramagnetic SPIONs assembly with a polymer layer will not fully screen magnetic field gradient.

Obtained magnetic layers were covered by a polystyrene (PS) layer using a spin-coating technique resulting fabrication of a flat polymeric surface (with roughness $R_q = 0.21 \pm 0.06$ nm) with the incorporated, any-shape, hidden magnetic pattern. Optimization of the spin-coating method was limited to changes in rotation speed only, leaving PS spin-coating time (45 s) and PS solution concentration (120 mg/ml) constant. Starting parameter of 2500 rpm turned out to be too fast, obtained PS coating layer was not homogeneous enough, preventing SPIONs pattern to be covered completely (see Fig. 1.C.2.). Reducing the rotation speed to 2000 rpm still did not result in complete coverage of patterned substrate (Fig. 1.C.3.). Reducing rotation speed to 1500 rpm allowed to produce flat and homogeneous layer, covering the SPIONs pattern completely (Fig. 1.C.4). From the application point of view of the next step, the deposition of the second layer of SPIONs, it is important that the newly prepared composite PS layer has magnetic properties. Moreover, the magnetic field lines should coincide with the shape of the underlying pattern, hidden under the PS coating. As it is shown in Fig. 2.C., the usually non-magnetic PS layer shows in the MFM phase image a clear magnetic response coming from the magnetized SPIONs arranged in a pattern of parallel stripes placed under the polymeric coating.

3.3. *Characterization of SPIONs on PS surface with hidden magnetic template*

So far, it has been have proved that the composite layers have magnetic properties and the shape of the magnetic domains located under the flat surface of the polymer can be easily controlled. The next experimental step would be to study the interaction of magnetic nanoparticles with the surface of the composite. The second deposition of magnetic SPIONs on the PS surface with a hidden magnetic pattern was carried out by immersion in nanoparticles solution. To protect from unwanted shift no water and no gas flow were used during the cleaning procedure. To confirm our idea, we used optical microscopy working in dark field mode (DF) to verify the effectiveness of deposition of SPIONs enhanced by magnetic interactions not by electrostatic attraction, as it had place during the first deposition on the patterned polyelectrolyte. DF mode was chosen to avoid misinterpretation caused by the observation of SPIONs on a transparent PS coating, through which particles located directly under PS surfaces are also visible. In DF mode, based on the intensity of the light scattered on surface-bound nanoparticles, while maintaining identical measurement conditions, clear differences in surface coverage level can be found. As it is shown in Fig. 3.A. bare SPIONs on PEI-PSS-PEI pattern show clear and intense signal which, after covering the surface with a screening [49] thin layer of PS, loses its intensity (see Fig. 3.B.). The signal originating from PS surface-bound SPIONs after the second deposition becomes intense again, which can be seen in Fig. 3.C. In this case whole surface of spin-coated PS on silicon substrate, due to no magnetic pattern incorporated below, was densely covered with nanoparticles. Such result was expected because of the influence of long deposition time (24 h) for these well-defined, stable, and homogeneous nanoparticles. The presence of the magnetic pattern under the PS surface influences greatly the final outcome. Preferential spatial organization of new portion of SPIONs occurs. It happens due to magnetic interactions between magnetic nanoparticles and the hidden magnetic patterns bound to the underlying silicon surface. Pattern on the surface imitates the pattern below the surface. Of course, the pattern obtained during second deposition is not as clear as it was after the first stage. The reason for that lays in strong electrostatic interactions dominating the latter event, whereas at this stage magnetic interactions dominate, being additionally screened by the presence of the PS layer.

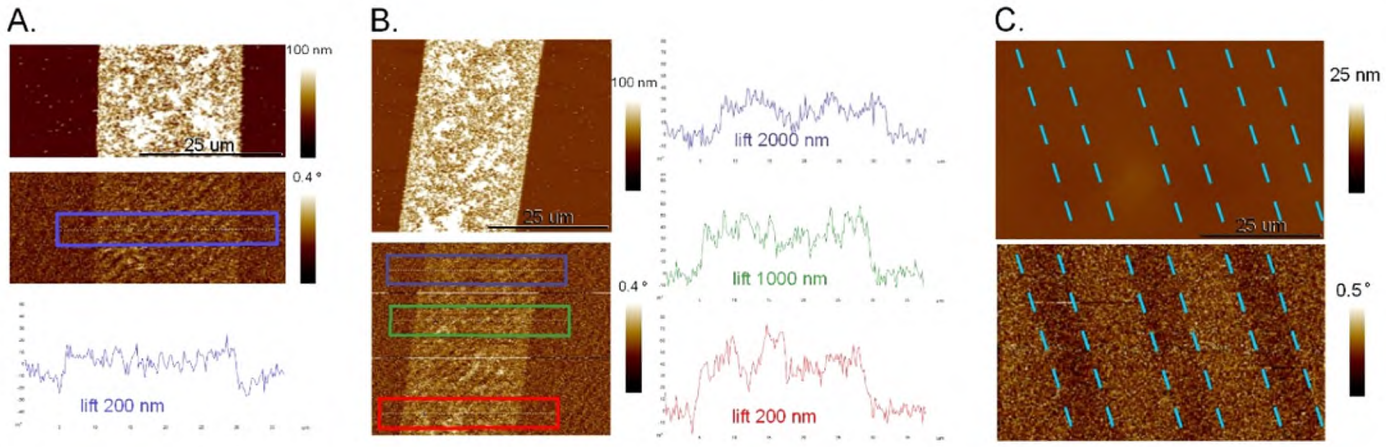

Fig. 2. Magnetic force microscopy images (top - topography, bottom – magnetic phase) of PEI-PSS-PEI with SPIONs patterns: A. bare pattern with untreated nanoparticles, B. bare pattern after 1 h at 80 °C (heat-treated nanoparticles) in the magnetic field with corresponding MFM phase cross-sections at different lift distances, C. PS coating above previously heat-treated patterns.

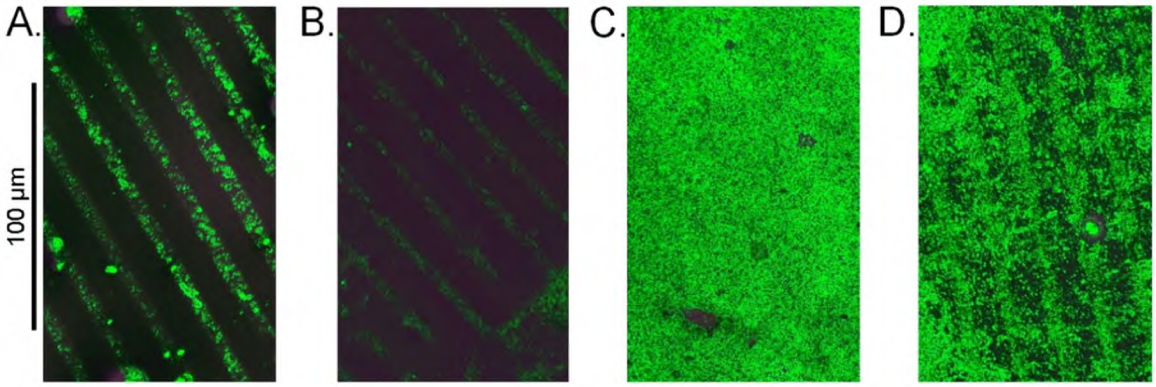

Fig. 3. Optical microscopy images in dark field mode: A. bare polyelectrolyte magnetic pattern, B. bare polyelectrolyte magnetic patterns covered by 1500 rpm spin-coated PS layer, C. SPIONs on bare 1500 rpm spin-coated PS layer, D. SPIONs on polyelectrolyte magnetic pattern.

Fig. 3.D. presents proof that the above concept is feasible and can be further optimized and improved.

The concept was confirmed on irregular shape patterns on flat silicon surface. The irregular shape of the pattern (Fig. 4.A.1.) was designed specifically to show the versatility of our method on shapes other than parallel stripes. As before SPIONs were deposited on the flat PS coating with (Fig. 4.B.3.) and without (Fig. 4.B.2.) magnetic pattern under the PS surface. As it is presented in the images from the optical microscope, the magnetic particles, as in the case of the pattern with stripes, were organized only on the surface with the magnetic pattern hidden under the polymer coating. What's more, the shape of the pattern, despite its difficult and confusing shape, was satisfactorily reproduced.

4. Conclusions

Our work presents a facile method of pattern-driven assembly of magnetic nanoparticles on flat polymeric surfaces. To fabricate polystyrene layer we used a cheap and commonly-used in many laboratories spin-coating technique. At the same time, most crucial, from the point of view of nanoparticles deposition processes, idea is hidden under the spin-coated polymer layer. Two-dimensional multi-layer polyelectrolyte (PEI-PSS-PEI) scaffolds stamped on smooth silicon surface have the necessary functionality to hold and spatially separate different types of nanoparticles. Although we used sets of parallel lines in the work, the stamped patterns can take any shape, depending on the design and concomitant photolithographic process of the creation of stamp itself. We covered the applied layer with magnetic nanoparticles (SPIONs), obtaining homogeneous layers of the thickness of 41.5 ± 3.1 nm and roughness below 12 nm, and to increase their magnetic response, we heated the whole surface to 80 °C. We proved that obtained magnetic patterned surfaces are strong enough to attract and organize magnetic material on their top, even when covered with polymeric layers. Phase

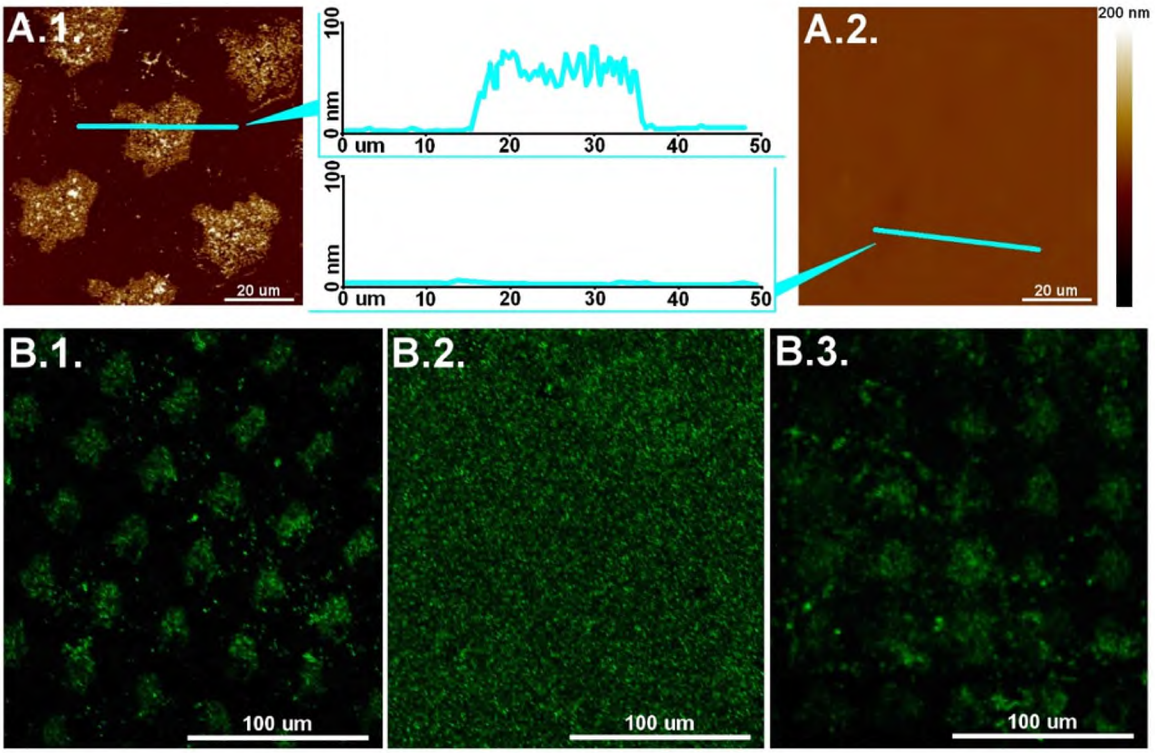

Fig. 4. AFM images (A.) with corresponding cross-sections of irregular shape pattern on flat silicon (1.) and the same pattern covered with 1500 rpm spin-coated PS layer (2.); optical microscopy images in dark field mode of irregular shape pattern (B.): 1. bare polyelectrolyte magnetic pattern, 2. SPIONs on bare 1500 rpm spin-coated PS layer, 3. SPIONs on polyelectrolyte irregular shape magnetic pattern.

images from magnetic force microscopy MFM confirmed strong magnetic interactions of both patterned samples and samples covered with a thin layer of polystyrene. Moreover, using optical and atomic force microscopy we confirmed that controlled and oriented deposition of magnetic SPIONs on the top of polymer surface depends only on the strength of magnetic interactions between the pattern and nanoparticles, not on topography of the surface (roughness $R_q = 0.21 \pm 0.06$ nm) or Brownian motions. Presented approach can generate several application outcomes. Obtained composite nanoparticle-polymer layers can be used whenever precise spatial control over nanoparticle assemblies is needed – eg. for mixed magnetic/non-magnetic composite materials. As far as the limitations go, the patterns for large-surface ordering still pose a challenge, yet the refinements of stamping procedures should resolve this issue. Upon future improvement, both strength and quality of magnetic fields for any-shape magnets can contribute to object displacement techniques – such as in magnetic tweezers or similar. In such setups very precise control over magnetic field gradients in the vicinity of probing magnetic beads is crucial.

CRediT authorship contribution statement

T. Mazur: Conceptualization, Methodology, Writing – review & editing, Ł. Mazur: Methodology, Writing – original draft, M. Borkowski: Methodology, T. Kuciel: Methodology, M. Szuwarzyński: Conceptualization, Methodology, Writing – original draft, Writing – review & editing.

Declaration of Competing Interest

The authors declare that they have no known competing financial interests or personal relationships that could have appeared to influence the work reported in this paper.

Data availability

Data will be made available on request.

Acknowledgments

The authors would like to thank for the financial support to the National Science Centre (Sonata Grant no. 2018/31/D/ST5/02813). Moreover, the authors would like to thank prof. Marcin Sikora (ACMiN AGH) for all the inspiring discussions.

References

[1] S. Kinge, M. Crego-Calama, D.N. Reinhoudt, Self-assembling nanoparticles at surfaces and interfaces, ChemPhysChem 9 (2008) 20–42, https://doi.org/10.1002/cphc.200700475.
[2] M.K. Kim, B.G. Cha, J. Kim, Directed assembly of magnetic nanoparticles into centimeter scale wires for a 3D cell culture platform, Chem. Mater. 34 (2022) 4437–4445, https://doi.org/10.1021/acs.chemmater.2c00120.
[3] P.M. Price, W.E. Mahmoud, A.A. Al-Ghamdi, L.M. Bronstein, Magnetic drug delivery: where the field is going, Front. Chem. 6 (2018) 1–7, https://doi.org/10.3389/fchem.2018.00619.
[4] R. Kumar, A. Chauhan, S.K. Jha, B.K. Kuanr, Localized cancer treatment by radio-frequency hyperthermia using magnetic nanoparticles immobilized on graphene oxide: from novel synthesis to in vitro studies, J. Mater. Chem. B. 6 (2018) 5385–5399, https://doi.org/10.1039/c8tb01365a.
[5] G. Reiss, A. Hütten, Magnetic nanoparticles: applications beyond data storage, Nat. Mater. 4 (2005) 725–726, https://doi.org/10.1038/nmat1494.
[6] W. Górka-Kumik, P. Garbacz, D. Lachowicz, P. Dąbczyński, S. Zapotoczny, M. Szuwarzyński, J. Mater. Chem. B 8 (2020) 10172–10181, https://doi.org/10.1039/D0TB01853H.
[7] T.R. Polte, M. Shen, J. Karavitis, M. Montoya, J. Pendse, S. Xia, E. Mazur, D. E. Ingber, Nanostructured magnetizable materials that switch cells between life and death, Biomaterials 28 (2007) 2783–2790, https://doi.org/10.1016/j.biomaterials.2007.01.045.
[8] N.A. Frey, S. Peng, K. Cheng, S. Sun, Magnetic nanoparticles: synthesis, functionalization, and applications in bioimaging and magnetic energy storage, Chem. Soc. Rev. 38 (2009) 2532–2542, https://doi.org/10.1039/b815548h.
[9] J. Odrobińska, E. Gumieniczek-Chłopek, M. Szuwarzyński, A. Radziszewska, S. Fiejdasz, T. Straczek, C. Kapusta, S. Zapotoczny, Magnetically navigated core–shell polymer capsules as nanoreactors loadable at the oil/water interface, ACS Appl. Mater. Interfaces 11 (2019) 10905–10913, https://doi.org/10.1021/acsami.8b22690.
[10] M. Tadic, S. Kralj, Y. Lalatonne, L. Motte, Iron oxide nanochains coated with silica: synthesis, surface effects andmagnetic properties, Appl. Surf. Sci. 476 (2019) 641–646, https://doi.org/10.1016/j.apsusc.2019.01.098.
[11] M. Tadic, J. Lazovic, M. Panjan, S. Kralj, Hierarchical iron oxide nanocomposite: bundle-like morphology, magnetic properties and potential biomedical application, Ceram. Int. 48 (2022) 16015–16022, https://doi.org/10.1016/j.ceramint.2022.02.145.
[12] R.M. Erb, H.S. Son, B. Samanta, V.M. Rotello, B.B. Yellen, Magnetic assembly of colloidal superstructures with multipole symmetry, Nature 457 (2009) 999–1002, https://doi.org/10.1038/nature07766.
[13] A.R. Urbach, J.C. Love, M.G. Prentiss, G.M. Whitesides, Whitesides, Sub-100 nm confinement of magnetic nanoparticles using localized magnetic field gradients, J. Am. Chem. Soc. 125 (2003) 12704–12705, https://doi.org/10.1021/ja0378308.
[14] A.F. Demirörs, P.P. Pillai, B. Kowalczyk, B.A. Grzybowski, Colloidal assembly directed by virtual magnetic moulds, Nature 503 (2013) 99–103, https://doi.org/10.1038/nature12591.
[15] K.K. Kefeni, T.A.M. Msagati, B.B. Mamba, Ferrite nanoparticles: synthesis, characterisation and applications in electronic device, Mater. Sci. Eng. B Solid-State Mater. Adv. Technol. 215 (2017) 37–55, https://doi.org/10.1016/j.mseb.2016.11.002.
[16] A. Ali, T. Shah, R. Ullah, P. Zhou, M. Guo, M. Ovais, Z. Tan, Y.K. Rui, Review on recent progress in magnetic nanoparticles: synthesis, characterization, and diverse applications, Front. Chem. 9 (2021) 1–25, https://doi.org/10.3389/fchem.2021.629054.
[17] W. Zhao, Z. Huang, L. Liu, W. Wang, J. Leng, Y. Liu, Porous bone tissue scaffold concept based on shape memory PLA/Fe3O4, Compos. Sci. Technol. 203 (2021), 108563, https://doi.org/10.1016/j.compscitech.2020.108563.
[18] L. Mohammed, H.G. Gomaa, D. Ragab, J. Zhu, Magnetic nanoparticles for environmental and biomedical applications: a review, Particuology 30 (2017) 1–14, https://doi.org/10.1016/j.partic.2016.06.001.
[19] M. Barrow, A. Taylor, A.M. Fuentes-Caparrós, J. Sharkey, L.M. Daniels, P. Mandal, B.K. Park, P. Murray, M.J. Rosseinsky, D.J. Adams, SPIONs for cell labelling and tracking using MRI: magnetite or maghemite? Biomater. Sci. 6 (2018) 101–106, https://doi.org/10.1039/c7bm00515f.
[20] Z.R. Stephen, F.M. Kievit, M. Zhang, Magnetite nanoparticles for medical MR imaging, Mater. Today 14 (2011) 330–338, https://doi.org/10.1016/S1369-7021(11)70163-8.
[21] C.A. Ross, Patterned magnetic recording media, Annu. Rev. Mater. Sci. 31 (2001) 203–235, https://doi.org/10.1146/annurev.matsci.31.1.203.
[22] R.L. Edelstein, C.R. Tamanaha, P.E. Sheehan, M.M. Miller, D.R. Baselt, L. J. Whitman, R.J. Colton, The BARC biosensor applied to the detection of biological warfare agents, Biosens. Bioelectron. 14 (2000) 805–813, https://doi.org/10.1016/S0956-5663(99)00054-8.
[23] A.O. Adeyeye, N. Singh, Large area patterned magnetic nanostructures, J. Phys. D. Appl. Phys. 41 (2008), 153001, https://doi.org/10.1088/0022-3727/41/15/153001.
[24] H.B. Cho, M. Kanno, M. Lim, T. Nakayama, Y.H. Choa, Design and synthesis of barium ferrite-based nanocomposite films with highly regulated 3-D structures, Appl. Surf. Sci. 555 (2021), 149515, https://doi.org/10.1016/j.apsusc.2021.149515.
[25] A.V. Lebedev, S.S. Kantorovich, A.O. Ivanov, I.M. Arefyev, A.F. Pshenichnikov, Weakening of magnetic response experimentally observed for ferrofluids with strongly interacting magnetic nanoparticles, J. Mol. Liq. 277 (2019) 762–768, https://doi.org/10.1016/j.molliq.2018.06.001.
[26] M. Grzelczak, J. Vermant, E.M. Furst, L.M. Liz-marza, Directed self-assembly of nanoparticles, ACS Nano 4 (2010) 3591–3605, https://doi.org/10.1021/nn100869j.
[27] K.A. Mirica, F. Ilievski, A.K. Ellerbee, S.S. Shevkoplyas, G.M. Whitesides, Using magnetic levitation for three dimensional self-assembly, Adv. Mater. 23 (2011) 4134–4140, https://doi.org/10.1002/adma.201101917.
[28] B.B. Yellen, G. Friedman, Programmable assembly of colloidal particles using magnetic microwell templates, Langmuir 20 (2004) 2553–2559, https://doi.org/10.1021/la0352016.
[29] A. Nagornyi, V.I. Petrenko, M. Rajnak, I.V. Gapon, M.V. Avdeev, B. Dolnik, L. A. Bulavin, P. Kopcansky, M. Timko, Particle assembling induced by non-homogeneous magnetic field at transformer oil-based ferrofluid/silicon crystal interface by neutron reflectometry, Appl. Surf. Sci. 473 (2019) 912–917, https://doi.org/10.1016/j.apsusc.2018.12.197.
[30] B. Yellen, G. Friedman, A. Feinerman, Printing superparamagnetic colloidal particle arrays on patterned magnetic film, J. Appl. Phys. 93 (2003) 7331–7333, https://doi.org/10.1063/1.1555908.
[31] B.B. Yellen, O. Hovorka, G. Friedman, Arranging matter by magnetic nanoparticle assemblers, Proc. Natl. Acad. Sci. U. S. A. 102 (2005) 8860–8864, https://doi.org/10.1073/pnas.050040910.
[32] M. Szuwarzyński, Ł. Mazur, M. Borkowski, K. Maćkosz, K. Giżyński, T. Mazur, Enhanced assembly of nanoparticles as a facile method of surface-independent fabrication of conductive patterns, ACS Appl. Nano Mater. 5 (2022) 12711–12719, https://doi.org/10.1021/acsanm.2c02559.
[33] I. Lee, H. Zheng, M.F. Rubner, P.T. Hammond, Controlled cluster size in patterned particle arrays via directed adsorption on confined surfaces, Adv. Mater. 14 (2002) 572–577, https://doi.org/10.1002/1521-4095.

[34] Y. Xia, Y. Yin, Y. Lu, J. McLellan, Template-assisted self-assembly of spherical colloids into complex and controllable structures, Adv. Funct. Mater. 13 (2003) 907–918, https://doi.org/10.1002/adfm.200300002.
[35] Y. Yin, Y. Xia, Self-assembly of spherical colloids into helical chains with well-controlled handedness, J. Am. Chem. Soc. 8 (2003) 2048–2049, https://doi.org/10.1021/ja029408h.
[36] F. Li, D.P. Josephson, A. Stein, Colloids colloidal assembly: the road from particles to colloidal molecules and crystals, Angew. Chem. Int. Ed. 50 (2011) 360–388, https://doi.org/10.1002/anie.201001451.
[37] S.M. Taheri, M. Michaelis, T. Friedrich, B. Förster, M. Drechsler, F.M. Römer, P. Bösecke, T. Narayanan, B. Weber, I. Rehberg, S. Rosenfeldt, S. Förster, Self-assembly of smallest magnetic particles, Proc. Natl. Acad. Sci. U. S. A. 112 (2015) 14484–14489, https://doi.org/10.1073/pnas.1511443112.
[38] C.S. Lee, H. Lee, R.M. Westervelt, Microelectromagnets for the control of magnetic nanoparticles, Appl. Phys. Lett. 79 (2001) 3308–3310, https://doi.org/10.1063/1.1419049.
[39] Z. Yang, J. Wei, K. Gizynski, M.G. Song, B.A. Grzybowski, Interference-like patterns of static magnetic fields imprinted into polymer/nanoparticle composites, Nat. Commun. 8 (2017), https://doi.org/10.1038/s41467-017-01861-1.
[40] M. Szuwarzyński, K. Wolski, T. Kruk, S. Zapotoczny, Macromolecular strategies for transporting electrons and excitation energy in ordered polymer layers, Prog. Polym. Sci. 121 (2021), 101433, https://doi.org/10.1016/j.progpolymsci.2021.101433.
[41] Y. Huangfu, C. Lianga,1, Y. Han, H. Qiu, P. Song, L. Wang, J. Kong, J. Gu, Fabrication and investigation on the Fe3O4/thermally annealed graphene aerogel/epoxy electromagnetic interference shielding nanocomposites, Compos. Sci. Technol. 169 (2019) 70–75, https://doi.org/10.1016/j.compscitech.2018.11.012.
[42] G.A. Badini Confalonieri, V. Vega, A. Ebbing, D. Mishra, P. Szary, V.M. Prida, O. Petracic, H. Zabel, Template-assisted self-assembly of individual and clusters of magnetic nanoparticles, Nanotechnology 22 (2011), 285608, https://doi.org/10.1088/0957-4484/22/28/285608.
[43] K. Gaska, G. Kmita, A. Rybak, R. Sekula, K. Goc, C. Kapusta, Magnetic-aligned, magnetite-filled epoxy composites with enhanced thermal conductivity, J. Mater. Sci. 50 (2015) 2510–2516, https://doi.org/10.1007/s10853-014-8809-8.
[44] K. Goc, K. Gaska, K. Klimczyk, A. Wujek, W. Prendota, L. Jarosinski, A. Rybak, Influence of magnetic field-aided filler orientation on structure and transport properties of ferrite filled composites, J. Magn. Magn. Mater. 419 (2016) 345–353, https://doi.org/10.1016/j.jmmm.2016.06.046.
[45] L. Xue, H. Yanchun, A. Lijia, Surface morphology control of immiscible polymer-blend thin films, Polymer 44 (2003) 8155–8165, https://doi.org/10.1016/j.polymer.2003.10.012.
[46] M. Borkowski, Ł. Mazur, K. Maćkosz, T. Mazur, M. Szuwarzyński, Low roughness, elevated stiffness and thickness-modulated surface nanocomposites based on the controlled deposition of polystyrene nanoparticles, J. Mater. Res. Technol. 19 (2022) 2799–2809, https://doi.org/10.1016/j.jmrt.2022.06.031.
[47] G. Kania, U. Kwolek, K. Nakai, S.I. Yusa, J. Bednar, T. Wójcik, S. Chłopicki, T. Skórka, M. Szuwarzyński, K. Szczubiałka, M. Kępczyński, M. Nowakowska, J. Mater. Chem. B 3 (2015) 5523–5531, https://doi.org/10.1039/C5TB00182J.
[48] Weronika Górka, Tomasz Kuciel, Paula Nalepa, Dorota Lachowicz, Szczepan Zapotoczny, Michał. Szuwarzyński, Homogeneous embedding of magnetic nanoparticles into polymer brushes during simultaneous surface-initiated polymerization, Nanomaterials 9 (2019) 456, https://doi.org/10.3390/nano9030456.
[49] H.L. Zhang, Y. Xia, J.G. Gai, Ultrathin active layer for transparent electromagnetic shielding window, ACS Omega 3 (2018), 2765–277,acsomega.7b02033.